TRENDS IN SCIENCES 2025; 22(12): 10924
https://doi.org/10.48048/tis.2025.10924
RESEARCH ARTICLE

Pharmacological Evaluation of F45 on the Cardiovascular System Using *In Vitro*, *In Vivo* Models and Molecular Dockings

Ikbolkhon Abdurazakova[1,*], Anvar Zaynabiddinov[2], Izzatullo Abdullaev[3], Lazizbek Makhmudov[3], Ulugbek Gayibov[3], Sirojiddin Omonturdiev[3], Gafurjon Abdullaev[4], Madina Xolmirzayeva[2] and Sherzod Zhurakulov[5]

[1]*Fergana Medical Institute of Public Health, Fergana Region, Uzbekistan*
[2]*Andijan State University, Andijan Region, Uzbekistan*
[3]*A. S. Sadykov Institute of Bioorganic Chemistry of the Science Academy of Uzbekistan, Plant Cytoprotectors Laboratory and Pharamacology, Tashkent, Uzbekistan*
[4]*Namangan State University, Namangan Region, Uzbekistan*
[5]*Institute of the Chemistry of Plant Substances, Uzbekistan Academy of Sciences, Tashkent, Uzbekistan*

([*]Corresponding author's e-mail: abdurazakovaiqbolxon@gmail.com)

Received: 12 June 2025, Revised: 3 July 2025, Accepted: 10 July 2025, Published: 10 September 2025

Abstract

The current study investigated the vasorelaxant and antihypertensive potential of the novel compound F-45 through a combination of *in vitro*, *in vivo*, and *in silico* approaches. F-45 demonstrated significant relaxation of rat aortic rings pre-contracted with KCl and phenylephrine, suggesting its capacity to inhibit both voltage-dependent L-type Ca^{2+} channels and receptor-operated calcium entry mechanisms. At 70 µM, F-45 reduced KCl-induced contraction by 84.0% ± 1.3%, while 45 µM of F-45 inhibited phenylephrine-induced contraction by 78.0% ± 2.2%. Endothelium-denuded experiments confirmed that nitric oxide signaling contributes significantly to F-45-mediated vasorelaxation, with a 35.0% ± 2.4% reduction in relaxation observed after endothelial removal. Molecular docking studies revealed high binding affinities of F-45 for Ca^{2+}-ATPase (−8.6 kcal/mol) and Sodium\Calcium Exchanger (−6.8 kcal/mol), supporting its role in modulating calcium transport. *In vivo* experiments using tail-cuff plethysmography showed that 50 mg/kg of F-45 reduced SBP and DBP from 132.5 ± 12.3 and 94.3 ± 9.1 to 96.8 ± 9.4 and 65.3 ± 6.4 mmHg, respectively. In the adrenaline-induced hypertension model, F-45 decreased elevated SBP and DBP from 140.8 ± 14.2 and 104.3 ± 10.3 to 90.0 ± 8.7 and 61.5 ± 6.0 mmHg within 2 h. These findings suggested that F-45 is a promising candidate for further development as a natural antihypertensive agent with multimodal action.

Keywords: F45, Vasorelaxation, Calcium channels, Molecular docking, Tail-cuff

Introduction

Hypertension continues to pose a major global health challenge, significantly contributing to cardiovascular morbidity and mortality. Despite the wide range of antihypertensive drugs currently available, their effectiveness is often compromised by adverse side effects, drug resistance, and limited efficacy in certain patient populations. This highlights the urgent need for safer and more effective therapeutic alternatives. In this context, natural products have gained increasing attention as potential complementary or alternative treatments for managing cardiovascular conditions. Among these, polyphenols, flavonoids, and tannins are of particular interest due to their potent antioxidant, anti-inflammatory, and vasoregulatory effects, which may help in lowering elevated blood pressure [1,2]. These plant-derived compounds are known to influence essential vascular mechanisms, including endothelial function and the activity of

voltage-gated calcium (Ca^{2+}) channels, both of which play critical roles in regulating vascular smooth muscle tone and peripheral resistance. Given their central role in modulating vascular contraction and maintaining blood pressure homeostasis, voltage-gated Ca^{2+} channels represent a promising target for antihypertensive drug development [3,4]. However, the direct vascular effects and specific interactions of most natural compounds with calcium transport systems remain insufficiently characterized [5]. Accordingly, the present study aims to explore the antihypertensive potential of F45, a biologically active natural compound, through a comprehensive experimental framework. By integrating *in vitro*, *in vivo*, and *in silico* approaches, the modulatory effects of F45 was assessed on vascular smooth muscle calcium signaling, systemic arterial pressure, and its binding affinity to calcium transport-associated proteins. This multifaceted strategy seeks to elucidate the mechanism of action of F45 and provide a scientific basis for its development as a novel, plant-derived antihypertensive agent.

Materials and methods

Structure and general characteristics

One of the compounds utilized in this study is a brominated arylamine derivative, structurally related to tricyclic agents resembling phenothiazine frameworks. The molecule contains a 3,4-dimethoxyphenyl moiety, a bromine-substituted phenyl ring, and a primary amine group, present in the form of a hydrochloride salt. This salt form improved the compound's aqueous solubility and may enhance its pharmacological profile. The presence of electron-donating groups ($-OCH_3$) and an electron-withdrawing bromine substituent (-Br) contributes to the molecule's lipophilicity, membrane permeability, and potential receptor-binding affinity (**Figure 1**). Furthermore, the amino group enables interactions with biological targets, particularly those involved in cardiovascular or neuroactive pathways. The compound's pharmacological relevance is potentially associated with antihypertensive, antispasmodic, or vasodilatory activities. Subsequent chapters will explore it's *in vivo* effects on cardiovascular function using validated experimental models [6,7].

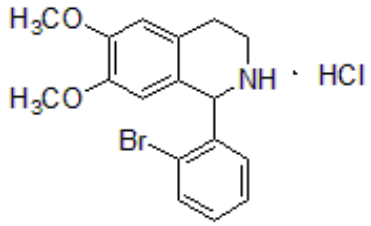

Figure 1 1-(2-bromophenyl)-2-(3,4-dimethoxyphenyl)ethylamine hydrochloride (F45).

Chemicals

Adrenaline-hydrochloride, Phenylephrine, phentolamine, and verapamil (≥ 98% purity) were purchased from Sigma-Aldrich (St. Louis, MO, USA).

Animal ethics

All preoperative and experimental procedures were carefully reviewed and approved by the Institutional Committee for Animal Use and Care. The animals were housed in a vivarium under standardized conditions, including a relative humidity of 55% - 65%, a controlled ambient temperature of 22 ± 2 °C, and unrestricted access to water and standard laboratory chow. All aspects of animal care and handling were conducted in full compliance with the European Directive 2010/63/EU, which governs the protection of animals used for scientific research. Ethical clearance for this study was granted by the Animal Ethics Committee of the Institute of Bioorganic Chemistry, Academy of Sciences of the Republic of Uzbekistan (Protocol No. 133/1a/h).

Tissue preparation

All surgical interventions were performed under sodium pentobarbital anesthesia to ensure the animals experienced no pain. The study utilized thoracic aorta tissue from healthy adult male Wistar rats, each weighing between 200 - 250 g. Euthanasia was conducted via cervical dislocation. Following thoracotomy, the aorta was carefully excised, with surrounding perivascular adipose and connective tissues

thoroughly removed. The cleaned aorta was then cut into vascular rings measuring 3 - 4 mm in length. These segments were transferred to a 5 mL organ bath containing Krebs-Henseleit physiological buffer, composed of (mM): NaCl 120.4, KCl 5, $NaHCO_3$ 15.5, NaH_2PO_4 1.2, $MgCl_2$ 1.2, $CaCl_2$ 2.5, glucose 11.5, and HEPES, adjusted to pH 7.4. In selected assays, a calcium-free Krebs solution supplemented with 1 mM EGTA was used to assess calcium-dependent vascular responses. Throughout the experiments, the buffer solution was continuously aerated with carbogen gas (95% O_2, 5% CO_2) and maintained at 37 °C using a DAIHAN ultrathermostatic water bath system [8].

Aortic-ring contraction studies

Aortic rings were suspended in a Radnoti isometric transducer system (USA) using platinum wire hooks and allowed to equilibrate for 60 min under standard physiological conditions. Each vascular segment was subjected to an initial preload tension of 1 g (10 mN). The contractile responses were recorded via an isometric transducer connected to a signal amplifier, with digital data acquisition carried out using a Go-link analog-to-digital converter linked to a computer system. Data acquisition and analysis were conducted using Origin Pro software, version 9 SR1 (EULA, Northampton, MA, USA). For statistical evaluation, the isometric tension (mN) generated by the aortic tissues was expressed as a percentage of the maximal contraction [9,10]. The functional activity of vascular smooth muscle was verified using an experimental setup based on the method described by Vandier *et al.* (2002). The 5 mL organ bath was integrated into a recirculating system containing Krebs-Henseleit solution (**Figure 2**). Bath temperature was precisely regulated via a thermostatic unit, and the solution was continuously aerated with a gas mixture of 95% O_2 and 5% CO_2. Isometric tension of the mounted aortic segments was continuously monitored using a Grass Instruments isometric force transducer (USA), with data visualization and recording facilitated by the GoLink amplifier and acquisition system [11].

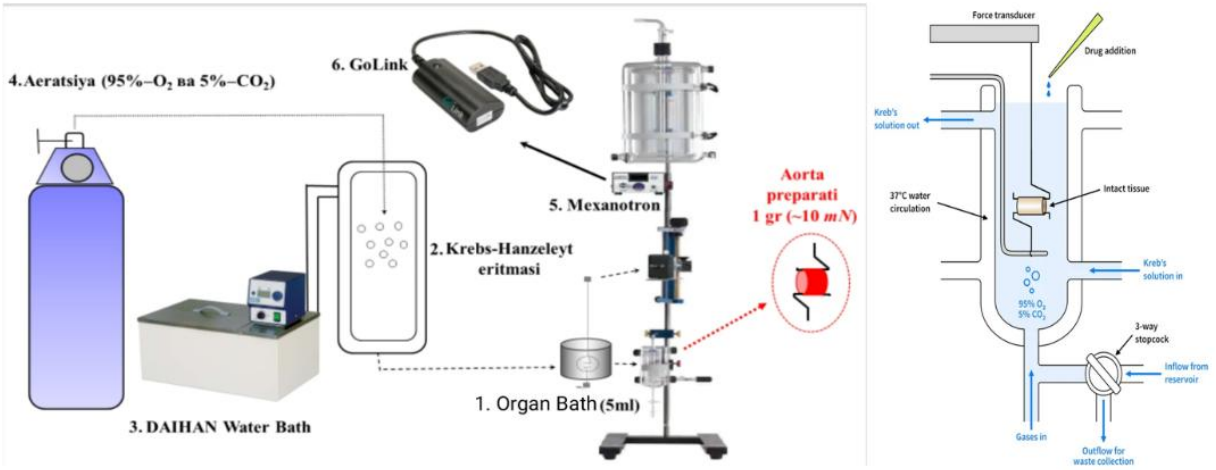

Figure 2 Diagram of the experimental setup used to monitor isometric contractions in isolated rat aortic vascular tissue. (1) The organ bath (5 mL) is connected to a dedicated reservoir for solution circulation. (2) Krebs-Henseleit solution is used to maintain physiological conditions. (3) A thermostat ensures stable temperature regulation. (4) The system is continuously aerated with a gas mixture containing 95% oxygen and 5% carbon dioxide. The aortic tissue is mounted within the experimental chamber for contraction assessment. (5) An isometric transducer (Grass Instrument, USA) captures mechanical responses, while (6) GoLink devices handle signal amplification and system integration.

Blood pressure measurements

Tail-cuff plethysmography was conducted using the Sistola system (Neurobotics, Russia) following a 3-day acclimatization period to minimize stress-induced variability (**Figure 3**). Blood pressure measurements were taken in triplicate during each session to ensure data reliability [12]. All experimental procedures were performed at the “BFM Pharmacology and Screening Laboratory” and the “Plant Cytoprotectors Laboratory” of the A. Sodikov Institute of Bioorganic Chemistry.

Data acquisition and analysis were performed using AcqKnowledge 4.2 software for the MP150 system (**Figure 3**).

Figure 3 The "Sistola" device (Neurobotics, Russia) used for non-invasive measurement of arterial blood pressure in rats via the tail artery.

Statistics

Statistical analysis and graphical representations were carried out using Origin Pro software, version 9 (USA). Vascular contractile responses were expressed as a percentage of the maximal contraction induced by either phenylephrine (10 mM) or potassium chloride (50 mM). Data are presented as the mean ± standard error from 4 to 6 independent experiments (n = 4 - 6). Paired t-tests were applied for comparisons within the same group, while unpaired t-tests were used to evaluate differences between experimental groups. A *p*-value of less than 0.05 was considered statistically significant.

Molecular docking "software and databases"

All software tools employed in this study were freely available for educational and academic use. Structural information on macromolecules involved in calcium signaling and regulation was obtained from the Protein Data Bank (PDB), a globally recognized repository of 3-dimensional biomolecular structures [13]. The selected target proteins included the L-type calcium channel Cav1.2 (PDB ID: 6jp5), R-type calcium channel Cav2.3 (PDB ID: 7xlq), sodium-calcium exchanger NCX1 (PDB ID: 8sgi), ryanodine receptor type 2 RyR2 (PDB ID: 5c33), and sarcoplasmic/endoplasmic reticulum Ca^{2+}-ATPase (SERCA, PDB ID: 6rb2). Additionally, the PubChem database was used to download reference compounds and the flavonoid ligands of interest. PubChem integrates extensive data on pharmacology, molecular targets, chemical structures, and biological pathways, and each DrugCard entry includes over 80 data fields related to small molecules and their protein targets (**Table 1**).

Visualization of PDB structures and docking outputs was performed using PyMOL (version 1.2), a Python-based molecular visualization tool [http://www.pymol.org]. Molecular docking was conducted with AutoDock 4.2, developed by The Scripps Research Institute (www.scripps.edu). Docking inputs and parameter settings were prepared using AutoDock Tools (ADT), an intuitive graphical interface designed for configuring and running docking simulations. AutoDock offers a reliable computational platform for predicting the binding modes and interactions between small molecules and macromolecular targets with known 3D structures [14].

Calculation of inhibition constant (Ki) from binding energy

In the molecular docking analysis, the strength of an interaction of a target protein and a ligand is usually quantified as the binding free energy (ΔG) in kilocalories per mole (kcal/mol) [5]. The binding energy can be utilized to determine the inhibition constant (Ki),

the binding affinity of a ligand, from a straightforward thermodynamic formula.

$$Ki = e^{\wedge} \frac{\Delta G \times 1{,}000}{R \times T} \quad (1)$$

where: Ki is the inhibition constant (in mol/L). ΔG is the binding free energy (in kcal/mol). R is the universal gas constant = 1.987 cal/(mol·K). T is the temperature in Kelvin (usually 298.15 K). The factor 1,000 converts kcal to cal.

Results and discussion

Investigation of the involvement of L-type and R-type Ca^{2+} channels in the vasorelaxant action of F45

It was well established that 50 mM KCl induced contraction in aortic smooth muscle primarily by activating voltage-dependent L-type calcium (Ca^{2+}) channels [15]. The elevation of extracellular potassium concentration leads to membrane depolarization, which alters the membrane potential and opens calcium channels, facilitating calcium influx into smooth muscle cells and triggering vasoconstriction. In this study, we investigated the vasorelaxant effects of the F45 compound on KCl-induced contractions in isolated rat aortic rings. Our results demonstrated that F45 induced concentration-dependent relaxation of pre-contracted aortic tissues. Specifically, within the 5 - 70 μM range, F45 significantly attenuated KCl (50 mM)-induced contractions, reducing contractile force from 15.0% ± 1.5% to 84.0% ± 1.3% compared to the control (**Figure 4(A)**). These findings suggest that F45 inhibits depolarization-induced calcium influx, likely through modulation or blockade of L-type Ca^{2+} channels on the vascular smooth muscle membrane. By suppressing extracellular calcium entry essential for contraction, F45 reduces intracellular calcium levels, thereby promoting vascular relaxation [16]. To further determine the specificity of this effect for L-type calcium channels, a comparative pharmacological approach was employed using verapamil, a well-known L-type Ca^{2+} channel blocker. Co-administration of F45 with a submaximal concentration of verapamil (0.1 μM), which only partially inhibited KCl-induced contractions, resulted in an additional 20.0% ± 1.7% relaxation, indicating a synergistic or additive effect between the 2 agents (**Figure 4(B)**). The IC_{50} value for F45 was calculated to be approximately 32.90 μM, supporting its pharmacological potency. In summary, these findings provide strong evidence that F45 exerts its vasorelaxant action predominantly by blocking or modulating voltage-gated L-type calcium channels, thereby inhibiting calcium influx and promoting smooth muscle relaxation. Its shared mechanism with verapamil highlights the potential of F45 as a promising candidate for the treatment of vascular disorders associated with calcium channel overactivity.

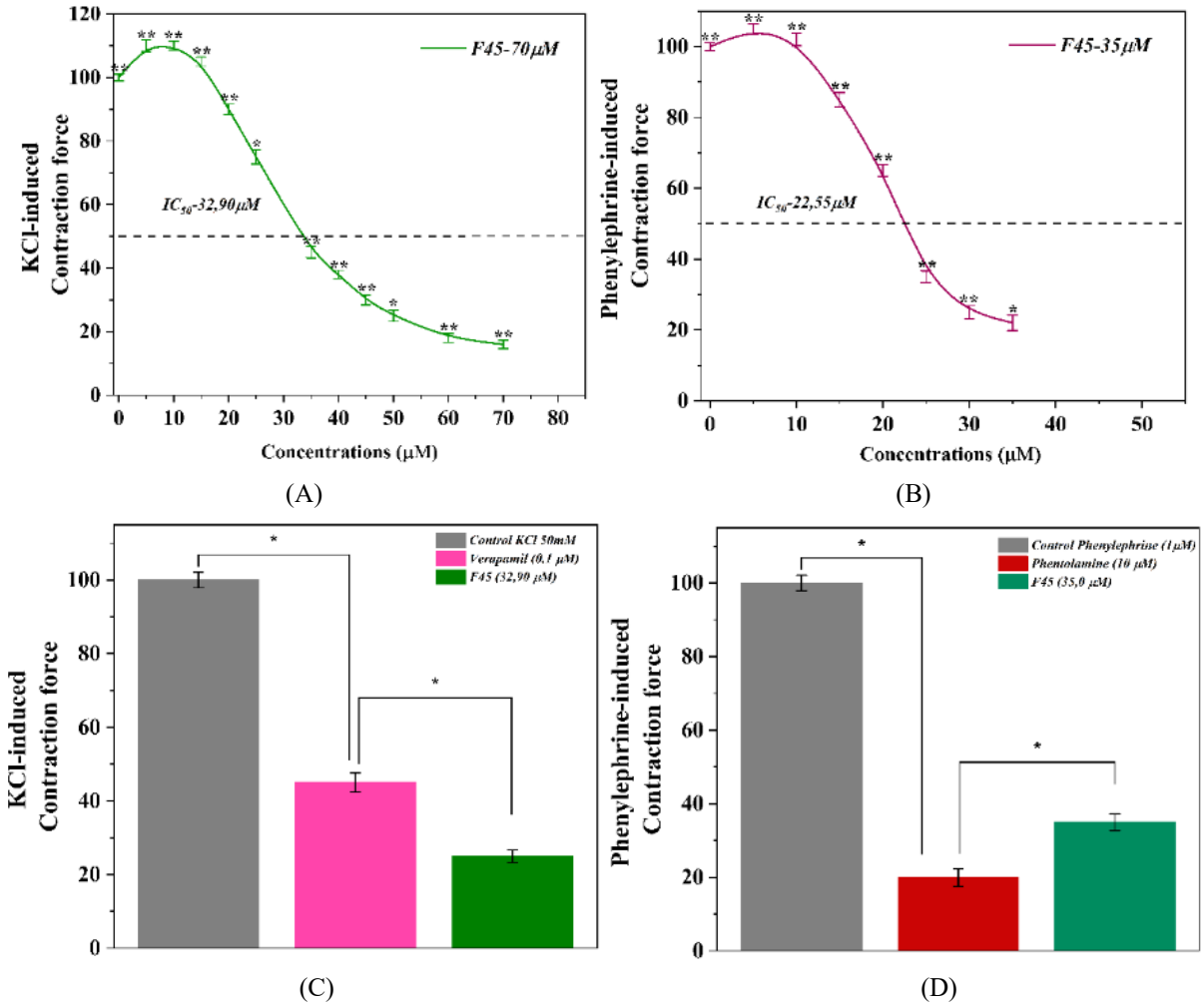

Figure 4 (A) Dose-dependent, linear vasorelaxant effect of compound F45 on KCl-induced contraction. (B) Comparison of F45 with the calcium channel blocker verapamil. (C) Effect of F45 on receptor-operated Ca^{2+} ion channels. (D) Confirmation of F45's mechanism using the α-adrenergic antagonist phentolamine. Data represent mean ± SEM, n = 3 - 4, $p < 0.05$.

It is well established that vascular smooth muscle contraction is regulated not only by voltage-gated L-type Ca^{2+} channels, but also by intracellular calcium signaling mechanisms, particularly those mediated by the sarcoplasmic reticulum (SR). Internal calcium stores and receptor-operated calcium channels (ROCCs) play a critical role in modulating intracellular calcium levels and, consequently, vascular tone [17]. To explore the potential involvement of F45 in modulating receptor-mediated calcium signaling, we examined its effect on phenylephrine (1 μM)-induced contractions in rat aortic rings. Phenylephrine, an α-adrenoceptor agonist, promotes vasoconstriction primarily by triggering calcium release from the SR and activating ROCCs on the plasma membrane. In our study, F45 significantly suppressed phenylephrine-induced contractions, demonstrating potent vasorelaxant activity. At the highest concentration tested (45 μM), F45 reduced the contractile response by 78.0% ± 2.2% compared to the control (**Figure 4(C)**). These findings suggested that F45 inhibits receptor-operated calcium entry and thereby reduces intracellular calcium levels and smooth muscle contraction [18]. To further elucidate this mechanism, comparative studies were conducted using phentolamine, a selective α-adrenoce.ptor antagonist, as well as known flavonoids that interfere with receptor-mediated calcium pathways. Phentolamine (10 μM) alone inhibited phenylephrine-induced contraction by 80.0% ± 2.6%. Notably, co-treatment with F45 (35 μM) and phentolamine led to an additional inhibition of 75.0% ± 2.2% (**Figure 4(D)**), indicating a possible additive or synergistic effect. This supports the

hypothesis that F45 interferes with α-adrenoceptor-mediated calcium signaling, likely by blocking ROCCs and possibly also by inhibiting downstream mobilization of intracellular calcium stores. Taken together, these results reinforce the conclusion that F45's vasorelaxant activity involves not only the inhibition of voltage-gated L-type Ca^{2+} channels but also significant modulation of receptor-operated calcium influx mechanisms, contributing to its overall antihypertensive potential [19].

A study on how endothelial mechanisms mediate the relaxant response elicited by A-51

The vascular endothelium plays a critical role in regulating vascular tone by releasing local mediators, with nitric oxide (NO) being the primary vasodilator produced by endothelial cells. When the endothelium is structurally or functionally compromised - a condition referred to as endothelial dysfunction (ED) - it becomes a major contributing factor in the development of cardiovascular diseases, including hypertension and atherosclerosis [20,21].

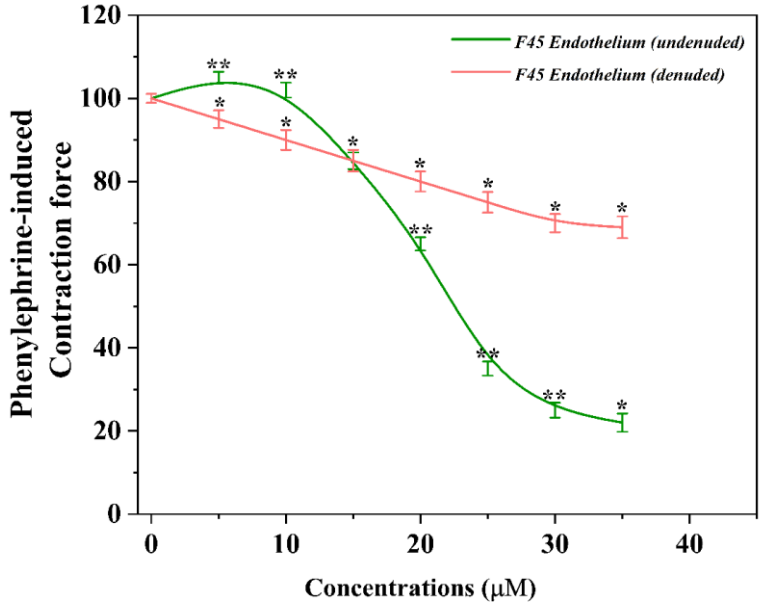

Figure 5 Relaxant effect of F45 on the contraction induced by Phe 1 μM in the undenuded and denuded of the rat aortic blood vessel endothelial layer. Contraction force elicited by 1 μM Phe was taken as 100% of control. (*$p < 0.05$, **$p < 0.01$; n = 5).

Endothelial dysfunction (ED) arises from an imbalance between vasoconstrictive and vasodilatory mediators, often initiated by oxidative stress and influenced by modifiable risk factors such as smoking, poor diet, and metabolic disorders [22]. A key mediator of endothelial function is nitric oxide (NO), which is synthesized in endothelial cells from L-arginine by the enzyme endothelial nitric oxide synthase (eNOS). The activity of eNOS is dependent on calcium-calmodulin and is negatively regulated through its interaction with caveolin, a membrane-associated inhibitory protein. Physiological stimuli such as acetylcholine or bradykinin promote the dissociation of eNOS from caveolin, enhancing NO production. Notably, low-dose statins have also been shown to increase NO availability by disrupting the eNOS-caveolin complex, contributing to their vascular protective properties [23]. However, oxidative stress can significantly disrupt this pathway by increasing the production of reactive oxygen species (ROS), which degrade NO and thereby reduce its bioavailability and vasodilatory capacity. Under normal physiological conditions, NO promotes relaxation of vascular smooth muscle via the NO/cGMP/PKG signaling cascade, which lowers intracellular Ca^{2+} levels, resulting in vasodilation [24]. To determine whether the endothelium contributes to the vasorelaxant effects of F45, additional assays were conducted using endothelium-denuded aortic rings. Removal of the endothelium led to a significant reduction in F45-induced relaxation, with a loss of 35.0% ± 2.4% in

vasorelaxant activity (**Figure 5**). This observation indicates that the endothelium - and likely NO signaling - is a major contributor to the vascular relaxation mediated by F45.

Molecular docking study of F45 with aortic ion channels

To elucidate the molecular basis of the vasorelaxant effects observed *in vitro*, a series of molecular docking experiments were conducted using the F45 compound. These simulations aimed to assess the binding affinity and inhibitory potential (Ki values) of F45 with several key calcium-regulating ion channels implicated in vascular smooth muscle contraction. The docking results provided molecular-level insights consistent with the functional data obtained experimentally. F45 was docked against calcium-handling proteins including L-type calcium channel, R-type calcium channel (Cav2.3), Ryanodine receptor 2 (RyR2), SERCA (Sarcoplasmic/Endoplasmic Reticulum Ca^{2+}-ATPase), Ca^{2+}-ATPase, and the Na^{+}/Ca^{2+} exchanger (NCX). Docking results demonstrated binding energies ranging from −6.6 to −8.7 kcal/mol, reflecting varying degrees of interaction strength. The strongest affinities were observed for Ca^{2+}-ATPase and NCX (−6.6 kcal/mol), suggesting robust and potentially functional interactions [25]. Corresponding Ki values supported this trend, indicating high-affinity binding to these targets. These results support the hypothesis that F45 may exert its vasodilatory effect in part through intracellular calcium modulation, particularly via Ca^{2+}-ATPase and NCX, both essential for calcium clearance and vascular tone regulation. Docking simulations revealed a binding energy of −7.8 kcal/mol for F45 with the L-type Ca^{2+} channel, indicating strong affinity and thermodynamic stability (**Figure 6(A)**). The compound formed specific interactions with key residues likely involved in channel regulation, including hydrogen bonds with ASN F:395 and ASP A:598, a pi-anion interaction with ASP A:598, and alkyl and pi-alkyl interactions with ARG A:593 and LEU F:269. These interactions suggest that F45 may interfere with the channel's functional core, potentially modulating its activity and contributing to reduced calcium influx and vascular smooth muscle relaxation. F45 displayed a binding energy of −6.6 kcal/mol with the SERCA protein, indicating moderate affinity and a stable interaction. The compound formed multiple contacts with catalytically and structurally significant residues, including hydrogen bonds with GLU A:40, PRO A:124, and LYS A:120, pi-anion interactions with GLU A:125 and GLU A:121, and pi-alkyl and alkyl interactions with LYS A:141, ALA A:142, and ARG A:143. These findings suggest that F45 may engage the active site of SERCA, potentially modulating its activity and affecting intracellular Ca^{2+} sequestration (**Figure 6(B)**).

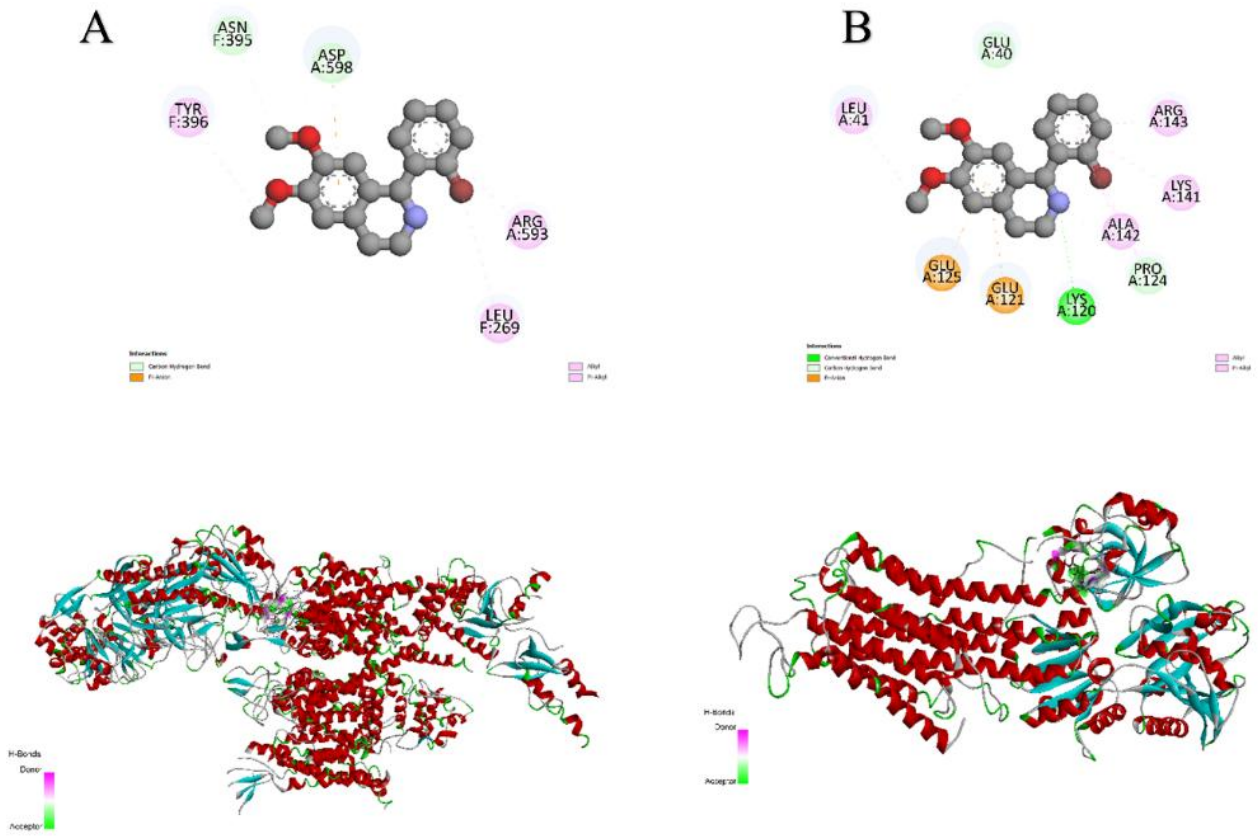

Figure 6 Molecular docking interactions of the F45 compound with calcium-regulating proteins. (A) Binding of F45 to the L-type calcium channel, showing hydrogen bonds with ASN F:395 and ASP A:598, and hydrophobic interactions with TYR F:396, ARG A:593, and LEU F:269. (B) Binding of F45 to SERCA (Sarcoplasmic/Endoplasmic Reticulum Ca^{2+}-ATPase), highlighting hydrogen bonding and hydrophobic contacts with GLU A:40, LYS A:120, GLU A:125, and ARG A:143. Bottom panels showed the overall protein-ligand complex structures and binding sites in 3D.

The docking analysis indicated a binding energy of −6.4 kcal/mol for F45 with RyR2, reflecting moderate affinity. F45 interacted with functionally relevant residues including a hydrogen bond with GLY B:710, pi-anion interactions with GLU A:701 and GLU A:711, and a pi-alkyl interaction with TYR B:703. Given the role of RyR2 in intracellular calcium release from the sarcoplasmic reticulum, these interactions suggest a potential modulatory role of F45 in calcium-induced calcium release (CICR) pathways, relevant in hypertensive pathophysiology (**Figure 7(A)**). F45 formed a highly stable complex with Ca^{2+}-ATPase, exhibiting a binding energy of −8.6 kcal/mol, the strongest among all tested targets. Key interactions included a pi-cation interaction with ARG A:559, a pi-pi stacked bond with PHE A:487, and pi-alkyl and alkyl contacts with LEU A:561, ALA A:516, and LYS A:492 (**Figure 7(B)**). These results highlight a strong and possibly inhibitory binding of F45 to Ca^{2+}-ATPase, suggesting interference with calcium extrusion mechanisms [26].

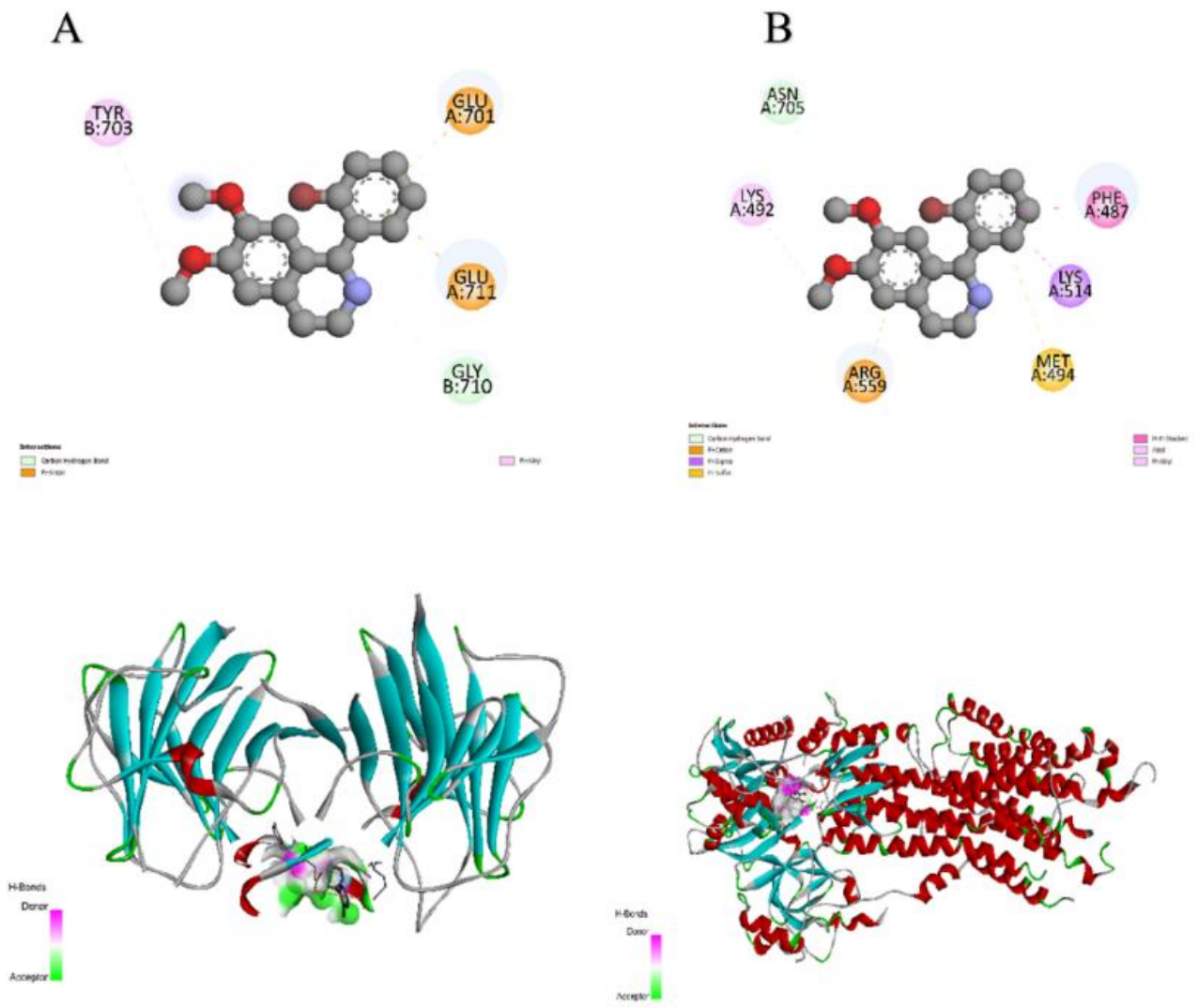

Figure 7 Molecular docking interactions of the F45 compound with calcium-regulatory targets. (A) Binding of F45 to the RyR2 (ryanodine receptor type 2), highlighting interactions with key residues including TYR B:703 (π-alkyl), GLU A:701 and GLU A:711 (pi-anion), and GLY B:710 (carbon hydrogen bond). (B) Binding of F45 to Ca^{2+}-ATPase, showing strong molecular contacts such as ARG A:559 (pi-cation), PHE A:487 (pi-pi stacking), and additional hydrophobic interactions with LYS A:492, LYS A:514, MET A:494, and ASN A:705. The lower panels show the 3D protein-ligand complex structures and interaction regions.

The docking analysis showed that F45 binds to NCX with a binding energy of −6.8 kcal/mol, indicating moderate affinity. The compound established key hydrophobic interactions with ARG A:63, ARG A:237, and VAL A:70. Given NCX's critical role in cellular calcium extrusion, particularly in cardiac and vascular smooth muscle cells, F45's interaction with this protein supports its potential in modulating Ca^{2+} homeostasis under hypertensive or stress conditions (**Figure 8(A)**).

As part of a broader screening effort, F45 was also docked with renin, a key enzyme in the renin-angiotensin system. The docking revealed a binding energy of −7.5 kcal/mol, indicating a strong and thermodynamically stable interaction. The binding was mediated by carbon-hydrogen bonding with ASP A:38, pi-pi stacking and T-shaped interactions with PHE A:119 and PHE A:124, and pi-alkyl and alkyl interactions with ALA A:303 and PHE A:124 (**Figure 8(B)**). This suggests that F45 may also exhibit regulatory potential in the renin-angiotensin pathway, providing an additional avenue for cardiovascular therapeutic application [27].

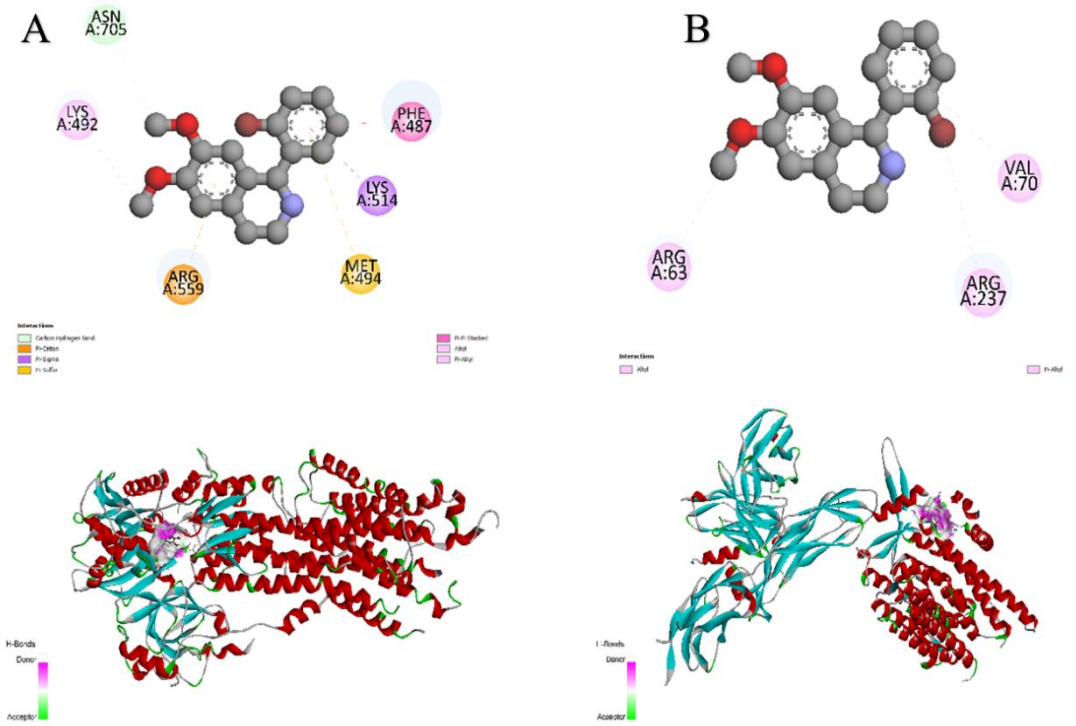

Figure 8 Molecular docking interactions of the F45 compound with renin and the Na^+/Ca^{2+} exchanger (NCX). (A) Binding of F45 to angiotensinogen-activating renin, showing pi-pi stacking (PHE A:487), pi-sulfur (MET A:494), pi-cation (ARG A:559), and additional alkyl interactions with LYS A:492, LYS A:514, and ASN A:705. (B) Interaction of F45 with NCX, highlighting pi-alkyl interactions involving ARG A:63, ARG A:237, and VAL A:70. Lower panels display the 3D structural context of each protein-ligand complex.

In conclusion, the molecular docking study revealed that F45 interacts with multiple calcium-handling proteins and potentially renin with moderate to high affinity. Its strongest predicted binding was observed with Ca^{2+}-ATPase and NCX, supporting its proposed mechanism of action in modulating calcium signaling and promoting vasorelaxation. These computational findings align with *in vitro* results and offer a mechanistic rationale for the development of F45 as a potential antihypertensive agent.

In vivo evaluation of dose-dependent blood pressure modulation by F-45 using the tail-cuff method

Dose-dependent blood pressure-lowering effect of F-45

Prior to the experiment, the baseline systolic blood pressure (SBP) and diastolic blood pressure (DBP) in the 25 mg/kg group were 105.0 ± 10.0 and 78.3 ± 7.6 mmHg, respectively (**Table 1**). In the 50 mg/kg group, baseline SBP and DBP were measured at 132.5 ± 12.3 and 94.3 ± 9.1 mmHg, respectively (**Figure 9(A)**). Following administration of F-45, blood pressure dynamics were monitored over a 3-hour period [28].

Table 1 *In vivo* evaluation of the antihypertensive activity of the F-45 compound.

	mg/kg	Baseline		1 h		2 h		3 h	
		SBP	DBP	SBP	DBP	SBP	DBP	SBP	DBP
F45	25	105.0 ± 10.0	78.3 ± 7.6	98.5 ± 8.9	63.3 ± 6.2	89.8 ± 8.7	65.5 ± 6.2	132.5 ± 12.8	95.8 ± 9.3
	50	132.5 ± 12.3	94.3 ± 9.1	97.5 ± 9.5	70.8 ± 6.3	97.8 ± 9.8	66.3 ± 6.2	96.8 ± 9.4	65.3 ± 6.4

In the 25 mg/kg group, SBP decreased sharply to 98.5 ± 8.9 mmHg and DBP to 63.3 ± 6.2 mmHg within the first hour. In the second hour, SBP and DBP further decreased to 89.8 ± 8.7 and 65.5 ± 6.2 mmHg, respectively. However, by the third hour, blood pressure values rebounded, reaching 132.5 ± 12.8 mmHg (SBP) and 95.8 ± 9.3 mmHg (DBP). In contrast, the 50 mg/kg group showed a more sustained effect. In the first hour, SBP and DBP dropped to 97.5 ± 9.5 and 70.8 ± 6.3 mmHg, respectively [29]. In the second hour, these values slightly decreased further to 97.8 ± 9.8 mmHg (SBP) and 66.3 ± 6.2 mmHg (DBP). By the third hour, blood pressure levels remained stable at 96.8 ± 9.4 mmHg (SBP) and 65.3 ± 6.4 mmHg (DBP) (**Figure 9(B)**).

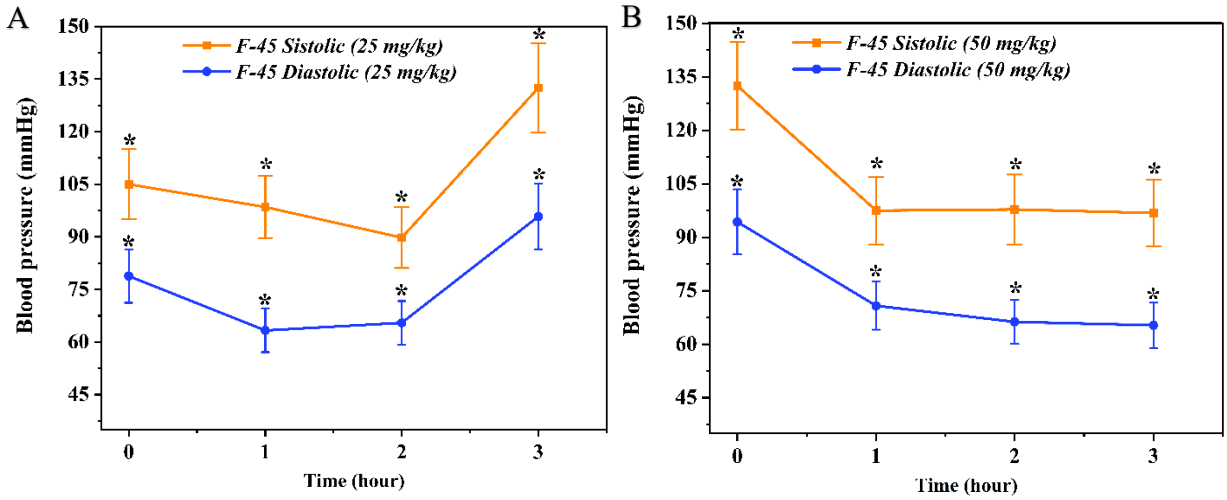

Figure 9 Evaluation of the effect of F-45 on systolic (SBP) and diastolic (DBP) blood pressure at doses of 25 mg/kg (A) and 50 mg/kg (B). Data are presented as mean ± standard deviation (n = 4). Statistical significance: $p > 0.05$.

These results indicated that F-45, particularly at a 50 mg/kg dose, exhibited a significant and sustained antihypertensive effect. This supports its potential as a promising candidate for further investigation as an antihypertensive agent in experimental models of hypertension.

Evaluation of the antihypertensive activity of F-45 in an adrenaline-induced hypertensive rat model

In this study, the antihypertensive potential of the compound F-45 was evaluated using an adrenaline-induced hypertension model in rats (**Table 2**). The experimental design began with the determination of an effective dose, with 50 mg/kg selected as the optimal working concentration based on preliminary screening. Subsequent *in vivo* assessments were conducted using this dose. Rats were randomly assigned into 3 groups: A control group and an F-45 treatment group, each consisting of 4 animals. All experimental procedures were carried out under standard biological protocols [30].

Table 2 *In vivo* antihypertensive activity of F-45 compounds (M ± m; n = 4).

Blood pressure (mmHg)		Control	F45, 50-mg/kg
Baseline	SBP	106.3 ± 10.5	92.5 ± 7.4
	DBP	76.8 ± 7.4	71.8 ± 6.2
Adrenaline 30-minute	SBP	160.5 ± 16.3	140.8 ± 14.2
	DBP	119.5 ± 11.8	104.3 ± 10.3
1 h	SBP	117.8 ± 11.6	101.8 ± 10.0
	DBP	98.8 ± 9.8	77.8 ± 7.6

Blood pressure (mmHg)		Control	F45, 50-mg/kg
2 h	SBP	125.5 ± 12.5	90.0 ± 8.7
	DBP	100.0 ± 10.1	61.5 ± 6.0
3 h	SBP	119.3 ± 11.8	96.3 ± 8.9
	DBP	94.0 ± 9.2	65.0 ± 6.3

At the start of the experiment, baseline blood pressure values were measured in normotensive rats: Systolic blood pressure (SBP) was 92.5 ± 7.4 mmHg and diastolic blood pressure (DBP) was 71.8 ± 6.2 mmHg. Upon administration of adrenaline, a hypertensive state was induced, with SBP rising to 140.8 ± 14.2 mmHg and DBP to 104.3 ± 10.3 mmHg. Immediately following this, F-45 was administered intravenously via the tail vein at a dose of 50 mg/kg, and blood pressure changes were monitored over a period of 3 h [31].

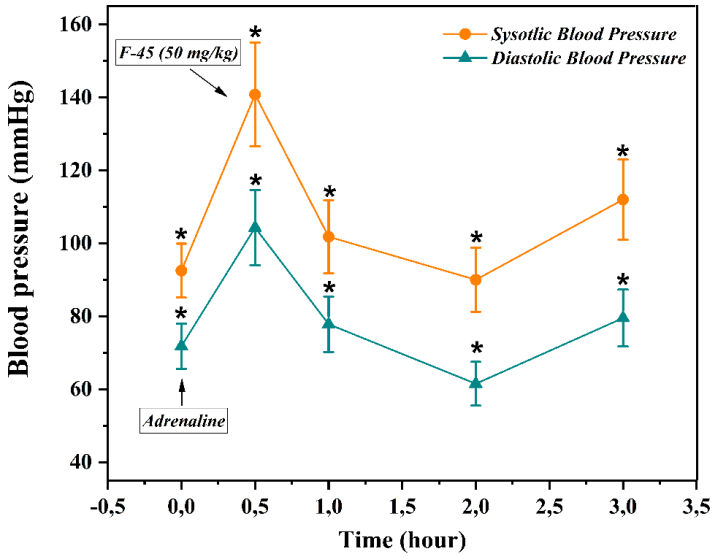

Figure 10 Evaluation of the effect of F-45 at a dose of 50 mg/kg on blood pressure in an adrenaline-induced hypertension model. SBP - systolic blood pressure; DBP - diastolic blood pressure. Data are presented as mean ± standard deviation (n = 4); $p > 0.05$.

Within the first hour, a pronounced antihypertensive effect was observed, with SBP decreasing to 101.8 ± 10.0 mmHg and DBP to 77.8 ± 7.6 mmHg. This trend continued into the second hour, where SBP dropped further to 90.0 ± 8.7 mmHg and DBP to 61.5 ± 6.0 mmHg. By the third hour, a partial rebound in blood pressure was observed, with SBP reaching 112.0 ± 11.0 mmHg and DBP stabilizing at 79.5 ± 7.8 mmHg (**Figure 10**). These results suggest that F-45 exerts a rapid and potent blood pressure-lowering effect in hypertensive conditions, followed by a moderate stabilization phase. The partial increase in blood pressure observed at the third hour indicated that the compound may have a short duration of action [32]. Nonetheless, the overall findings demonstrate that F-45 possesses clear antihypertensive activity in an adrenaline-induced hypertension model and supports its potential as a candidate for further investigation in the development of short-acting antihypertensive agents.

Discussion

This comprehensive study provided multiple lines of evidence supporting the antihypertensive and vasorelaxant activity of the F-45 compound. *In vitro* findings demonstrate that F-45 effectively attenuates KCl-induced contractions in a dose-dependent manner, primarily through inhibition of L-type Ca^{2+} channels. The synergistic interaction observed with verapamil

strengthens the hypothesis of shared or complementary mechanisms. Furthermore, F-45 significantly inhibited phenylephrine-induced contractions, indicating interference with receptor-operated calcium channels and possibly intracellular calcium stores. The additive effect with phentolamine highlights its role in modulating α-adrenoceptor-mediated calcium signaling. The endothelial mechanism was also shown to be a key contributor to the vasodilatory action of F-45. The significant reduction in vasorelaxation following endothelial removal supports the involvement of nitric oxide (NO)-mediated pathways, likely via eNOS activation. These results align with known vascular mechanisms, where NO induces vasodilation by reducing intracellular Ca^{2+} through the NO/cGMP/PKG pathway. Molecular docking studies provided additional mechanistic insights, revealing moderate to strong binding affinities of F-45 to multiple calcium-handling proteins. The strongest interactions were observed with Ca^{2+}-ATPase and NCX, both central to calcium clearance and vascular tone maintenance. The interaction with renin also suggested potential modulation of the renin–angiotensin system. The alignment of docking results with *in vitro* pharmacology underscores the dual membrane and intracellular targets of F-45. *In vivo* studies confirmed the antihypertensive effect of F-45. Tail-cuff measurements showed that the 50 mg/kg dose produced a stable reduction in systolic and diastolic blood pressure over 3 h. The adrenaline-induced hypertensive model further demonstrated the compound's rapid and potent blood pressure-lowering effect, although a partial rebound in the third hour suggests a relatively short duration of action. Together, these findings provide compelling evidence for the therapeutic potential of F-45 in the management of hypertension.

Conclusions

F-45 has been shown to exert potent vasorelaxant and antihypertensive effects through a multimodal mechanism involving inhibition of voltage-gated and receptor-operated Ca^{2+} channels, modulation of endothelial nitric oxide signaling, and interference with intracellular calcium regulation pathways. Its high binding affinity for Ca^{2+}-ATPase, NCX, and renin further supports its pharmacological relevance. *In vivo* data validate its efficacy in both normotensive and hypertensive states. These findings suggest that F-45 represents a promising lead compound for the development of a short-acting, nature-based antihypertensive therapeutic agent. Further studies focusing on its pharmacokinetics, chronic efficacy, and safety profile are warranted to advance its clinical potential.

Declaration of Generative AI in Scientific Writing

Only minimal assistance was used from QuillBot for paraphrasing selected sentences. All scientific content, interpretation, and conclusions were developed independently by the authors.

CRediT Author Statement

Ikbolkhon Abdurazakova designed and performed the experiments. **Anvar Zaynabiddinov** supervised the overall research activities and provided critical guidance. **Izzatullo Abdullaev** contributed to manuscript drafting and literature analysis. **Lazizbek Makhmudov** conducted the *in vivo* pharmacological experiments. **Ulugbek Gayibov** performed the *in silico* studies and data interpretation. **Sirojiddin Omonturdiev** carried out the *in vitro* assays. **Gafurjon Abdullaev** supervised the study and contributed to methodological validation. **Madina Xolmirzayeva** co-supervised the project and reviewed the manuscript. **Sherzod Zhurakulov** synthesized the studied compounds and ensured chemical purity.

References

[1] M Di Cesare, P Perel, S Taylor, C Kabudula, H Bixby, TA Gaziano, DV McGhie, J Mwangi, B Perva, J Narula, D Pineiro and FJ Pinto. The heart of the world. *Global Heart* 2024; **19(1)**, 11.

[2] I Abdullaev, U Gayibov, S Omonturdiev, S Fotima, S Gayibova and T Aripov. Molecular pathways in cardiovascular disease under hypoxia: Mechanisms, biomarkers, and therapeutic target. *The Journal of Biomedical Research* 2025; **39(3)**, 254-269.

[3] CJ Hutchings, P Colussi and TG Clark. Ion channels as therapeutic antibody targets. *mAbs* 2019; **11(2)**, 265-296.

[4] AA Abdullaev, DR Inamjanov, DS Abduazimova, SZ Omonturdiyev, UG Gayibov, SN Gayibova and TF Aripov. *Silybum Mariánum's* impact on

physiological alterations and oxidative stress in diabetic rats. *Biomedical and Pharmacology Journal* 2024; **17(2)**, 1291-1300.

[5] BK Joseph, KM Thakali, CL Moore and SW Rhee. Ion channel remodeling in vascular smooth muscle during hypertension: Implications for novel therapeutic approaches. *Pharmacological Research* 2013; **70(1)**, 126-138.

[6] O Gaibullayeva, A Islomov, D Abdugafurova, B Elmurodov, B Mirsalixov, L Mahmudov, I Adullaev, K Baratov, S Omonturdiev and S Sa'dullayeva. *Inula helenium* L. root extract in sunflower oil: Determination of its content of water-soluble vitamins and immunity-promoting effect. *Biomedical and Pharmacology Journal* 2024; **17(4)**, 2729-2737.

[7] AQQ Azimova, AX Islomov, SA Maulyanov, DG Abdugafurova, LU Mahmudov, IZ Abdullaev, AS Ishmuratova, SQ Siddikova and IR Askarov. Determination of vitamins and pharmacological properties of *Vitis vinifera* L. plant fruit part (mixed varieties) syrup-honey. *Biomedical and Pharmacology Journal* 2024; **17(4)**, 2779-2786.

[8] AV Mahmudov, OS Abduraimov, SB Erdonov, UG Gayibov and LY Izotova. Bioecological features of *Nigella sativa* L. in different conditions of Uzbekistan. *Plant Science Today* 2022; **9(2)**, 421-426.

[9] OS Zoirovich, AIZ Ugli, ID Raxmatillayevich, ML Umarjonovich, ZM Ravshanovna and G Sabina. The effect of Ájuga Turkestánica on the rat aortic smooth muscle ion channels. *Biomedical and Pharmacology Journal* 2024; **17(2)**, 1213-1222.

[10] D Inomjonov, I Abdullaev, S Omonturdiev, A Abdullaev, L Maxmudov, M Zaripova, M Abdullayeva, D Abduazimova, S Menglieva, S Gayibova, M Sadbarxon, U Gayibov and T Aripov. *In vitro* and *In vivo* studies of *Crategus* and *Inula helenium* extracts: Their effects on rat blood pressure. *Trends in Sciences* 2025; **22(3)**, 9158.

[11] A Abdullaev, I Abdullaev, A Bogbekov, U Gayibov, S Omonturdiev, S Gayibova, M Turahodjayev, K Ruziboev and T Aripov. Antioxidant potential of *Rhodiola heterodonta* extract: Activation of Nrf2 pathway via integrative *in vivo* and *in silico* studies. *Trends in Sciences* 2025; **22(5)**, 9521.

[12] HM Berman, J Westbrook, Z Feng, G Gilliland, TN Bhat, H Weissig, IN Shindyalov and PE Bourne. The protein data bank. *Nucleic Acids Research* 2000; **28(1)**, 235-242.

[13] H Zohny, J McMillan and M King. Ethics of generative AI. *Journal of Medical Ethics* 2023; **49(2)**, 79-80.

[14] M Iman, A Saadabadi and A Davood. Molecular docking analysis and molecular dynamics simulation study of ameltolide analogous as a sodium channel blocker. *Turkish Journal of Chemistry* 2015; **39(2)**, 10.

[15] J Palacios, D Asunción-Alvarez, D Aravena, M Chiong, MA Catalán, C Parra, F Cifuentes and A Paredes. A new oxime synthesized from *Senecio nutans* SCh. Bip (chachacoma) reduces calcium influx in the vascular contractile response in rat aorta. *RSC Advances* 2024; **14**, 9933-9942.

[16] J Striessnig, NJ Ortner and A Pinggera. Pharmacology of L-type calcium channels: Novel drugs for old targets? *Current Molecular Pharmacology* 2015; **8(2)**, 110-122.

[17] M Al-Khrasani, DA Karadi, AR Galambos, B Sperlagh and ES Vizi. The pharmacological effects of phenylephrine are indirect, mediated by noradrenaline release from the cytoplasm. *Neurochemical Research* 2022; **47(11)**, 3272-3284.

[18] UG Gayibov, SN Gayibova, DS Abduazimova, RN Rakhimov, HS Ruziboev, MA Xolmirzayeva, AE Zaynabiddinov and TF Aripov. Antioxidant and cardioprotective properties of polyphenolic plant extract of *Rhus glabra* L. *Plant Science Today* 2024; **11(3)**, 2348-1900.

[19] TF Aripov and UG Gayibov. Antiradical and antioxidant activity of the preparation "Rutan" from *Rhus coriaria* L. *Journal of Theoretical and Clinical Medicine* 2023; **4**, 164-170.

[20] AV Mahmudov, OS Abduraimov, SB Erdonov, AL Allamurotov, OT Mamatkasimov, UG Gayibov and LY Izotova. Seed productivity of *Linum usitatissimum* L. in different ecological conditions of Uzbekistan. *Plant Science Today* 2022; **9(4)**, 1090-1101.

[21] A Sandoo, JJCSV van Zanten, GS Metsios, D Carroll and GD Kitas. The endothelium and its role in regulating vascular tone. *The Open Cardiovascular Medicine Journal* 2010; **23(4)**, 302-312.

[22] PJ Tonge. Drug-target kinetics in drug discovery. *ACS Chemical Neuroscience Journal* 2018; **9(1)**, 29-39.

[23] S Sodiqova, S Kadirova, A Zaynabiddinov, I Abdullaev, L Makhmudov, U Gayibov, M Yuldasheva, M Xolmirzayeva, R Rakhimov, A Mutalibov and H Karimjonov. Channelopathy activity of A-41(Propyl ester of gallic acid): Experimental and computational study of antihypertensive activity. *Trends in Sciences* 2025 **22(9)**, 10496.

[24] M Zaripova, I Abdullaev, A Bogbekov, U Gayibov, S Omonturdiev, R Makhmudov, N Ergashev, G Jabbarova, S Gayibova and T Aripov, T. *In vitro* and *in silico* studies of Gnaphalium U. extract: Inhibition of α-amylase and α-glucosidase as a potential strategy for metabolic syndrome regulation. *Trends in Sciences* 2025 **22(8)**, 10098.

[25] UG Gayibov, EJ Komilov, RN Rakhimov, NA Ergashev, NG Abdullajanova, MI Asrorov and TF Aripov. Influence of new polyphenol compound from Euphorbia plant on mitochondrial function. *Journal of Microbiology Biotechnology and Food Science* 2019; **8(4)**, 1021-1025.

[26] S Shao and RS Hegde. Membrane protein insertion at the endoplasmic reticulum. *Annual Review of Cell and Developmental Biology* 2011; **27**, 25-56.

[27] EM Capes, R Loaiza and HH Valdivia. Ryanodine receptors. *Skelet Muscle* 2011; **1(1)**, 18.

[28] Y Umidakhon, B Erkin, G Ulugbek, N Bahadir and A Karim. Correction of the mitochondrial NADH oxidase activity, peroxidation and phospholipid metabolism by haplogenin-7-glucoside in hypoxia and ischemia. *Trends in Sciences* 2022; **19(21)**, 6260.

[29] MK Pozilov, U Gayibov, MI Asrarov, NG Abdulladjanova, HS Ruziboev and TF Aripov. Physiological alterations of mitochondria under diabetes condition and its correction by polyphenol gossitan. *Journal of Microbiology Biotechnology and Food Science* 2022; **12(2)**, e2224.

[30] AG Vakhobjonovna, KE Jurayevich, AIZ Ogli, EN Azamovich, MR Rasuljonovich and AM Islomovich. Tannins as modulators in the prevention of mitochondrial dysfunction. *Trends in Sciences* 2025 **22(8)**, 10436.

[31] Z Shakiryanova, R Khegay, U Gayibov, A Saparbekova, Z Konarbayeva, A Latif and O Smirnova. Isolation and study of a bioactive extract enriched with anthocyanin from red grape pomace (Cabernet Sauvignon). *Agronomy Research* 2023; **21(3)**, 1293-1303.

[32] U Gayibov, SN Gayibova, KP Ma'murjon, FS Tuxtaeva, UR Yusupova, GMK Djabbarova, ZA Mamatova, NA Ergashev and TF Aripov. Influence of quercetin and dihydroquercetin on some functional parameters of rat liver mitochondria. *Journal of Microbiology, Biotechnology and Food Sciences* 2021; **11(1)**, e2924.

[33] DG Harrison, M Bader, LO Lerman, G Fink, SA Karumanchi, JF Reckelhoff, MLS Sequeira-Lopez and RM Touyz. Tail-cuff versus radiotelemetry to measure blood pressure in mice and rats. *Hypertension* 2024; **81(1)**, 3-5.

[34] MR Zaripova, SN Gayibova, RR Makhmudov, AA Mamadrahimov, NL Vypova, UG Gayibov, SM Miralimova and TF Aripov. Characterization of *Rhodiola heterodonta* (Crassulaceae): Phytocomposition, antioxidant and antihyperglycemic activities. *Preventitive Nutrition Food Science* 2024; **29(2)**, 135-145.